EUROPEAN ORGANIZATION FOR NUCLEAR RESEARCH

CERN-EP/82-198
December 7th, 1982

THE PERFORMANCE OF A 16000 WIRE MINI-DRIFT MWPC SYSTEM

P. Chauvat, R. Cousins[1], K. Hayes, A.M. Smith
CERN, 1211 Geneva 23, Switzerland.

R. Bonino, J. Ellett, M. Medinnis, A. Russ, P.E. Schlein[2],
P. Sherwood, J.G. Zweizig
University of California*), Los Angeles, California 90024, USA

J. Alitti, B. Bloch-Devaux, A. Borg, J.B. Cheze, A. Diamant-Berger,
I. Giomataris, B. Pichard, F. Rollinger, M. Tararine, J. Zsembery.
Centre d'Etudes Nucleaires-Saclay, 91190 Gif-sur-Yvette, France.

Geneva, December 13, 1982

Abstract: The Mini-Drift chamber system and associated electronics employed in experiment R608 at the CERN-ISR are described. The performance of the system which utilizes 3mm spacing MWPCs produces a spatial resolution of σ = 180 μ under experimental conditions.

Submitted to the
XXI International Conference on High Energy Physics
Paris 26-31 July 1982

---

*) Supported in part by the U.S. National Science Foundation

[1]) Now at University of California, Los Angeles

[2]) also at CERN, Geneva

1. INTRODUCTION

While it has been believed since the early days of Multi-Wire- Proportional-Chamber usage that spatial information was available in the arrival time of chamber pulses [G. Charpak et al.-NIM 62, 235(68)], no full-scale experiment has, to our knowledge, made use of this information to improve resolution. This was due partly to the vast amount of electronics necessary to time-digitize signals from a typical experiment with tens of thousands of channels, and partly to the advent of larger cell drift chambers.

Nonetheless, in experimental situations with high rates or high spatial density of particles, one would like to retain the narrow cells of MWPC systems while achieving the σ = 200 μ resolution typical of drift chambers.

In our application at the CERN Intersecting-Storage-Rings, we were faced with a relatively high rate ($\approx 10^6$/sec) and particle density in the forward direction of pp and pp interactions. Moreover, the available magnetic field integral was low ($\approx$0.3 Tm), so that σ = 200 μ was needed for good momentum resolution. Thus, the Mini-Drift solution was chosen.

The NEVIS group of Sippach et al. pioneered in the development of a compact 16 channel 6-bit TDC using ECL electronics. In the system described here, we have carried on in this direction in developing a 32-channel 4-bit ECL TDC module. We have also developed a fast readout system and associated multiplicity logic which has a data flow rate of several hundred Megabytes per second. In particular, we have constructed and gained experience with a large system consisting of 514 32-channel amplifier-cable-TDC units.

Besides the electronics demands made by Mini-Drift, the inherent problem of left-right ambiguity resolution is exaggerated because the tracks are always close to the nearest sense wire (1.5 mm in our case). Redundant measurements are necessary to insure a high probability of correct solutions.

The charged-particle spectrometer of experiment R608 at the CERN ISR has been in operation since February 1981. The system performs well even at the highest ISR luminosities, with good multi-track efficiency and momentum resolution. The global spatial resolution, measured to be σ = 180 μ, results in momentum resolution of $\sigma p/p$ = 5.8 % AT 26.7 Gev/c.

2. SPECTROMETER AND CHAMBER CONSTRUCTION

The layout of the double septum magnetic spectrometer is shown in figure 1. The wire chambers of the spectrometer, constructed at Saclay, consist of five pairs of MWPC packs placed above and below the ISR beam pipe with 3 pairs upstream and 2 pairs downstream of the magnet. The chambers above the pipe and those below the pipe can be thought of as constituting two independent spectrometers, which we refer to as the UP and DOWN spectrometers, respectively. There are 16448 wires in the system.

Each chamber pack has four planes of wires, X, X', Y and U, the latter being inclined at approximately 37 degrees to the vertical. The X' and X wires are vertical and are displaced horizontally with respect to one another by 1/4, 1/2 or 3/4 of the 3 mm wire spacing.

The chambers are constructed with 7 mm between a sense wire plane and each of its neighboring cathode planes. The cathode planes are constructed of mylar with graphite coating on both sides. The chambers are operated with the cathode planes at -3.3 kV giving the potential distribution shown in Figure 2. This distribution is typical of MWPCs, and is different from the standard drift chamber field configuration. In order for the pulse arrival time to measure the distance in the sense wire plane between a sense wire and the traversal point of a track in that plane, the ionization electron nearest the sense wire plane must not be too far from that plane. With 40 or more ionization centers per track traversal and with electronics sensitive to the first electrons, this condition appears to be satisfied. Clearly the velocity is not near saturation in the well-known low-field region midway between the wires but this appears to pose no problem as discussed in section 1.4 below.

The chambers are filled with 60% argon, 39% isobutane and 1% of a mixture of argon containing 1% freon. The argon is bubbled through isopropyl alcohol at 4 degrees celsius. While we have not made extensive tests of the optimal gas mixtures for this application, it is noteworthy that the desired results have been obtained with this rather typical unexotic gas mixture.

3. CHAMBER ELECTRONICS

The amplifier cards consist of four amplification stages each utilizing a Motorola MC10115 Emitter-Coupled-Logic (ECL) integrated circuit, followed by a MC10116 line-driver stage. The inputs of the 10116's are biassed to 200 mv so that an amplified chamber signal of -300 mv produces a full differential logic swing at the output. With four cascaded stages of amplification, a small change from the nominal VEE of -5.2 V allows the overall gain to be adjusted from a maximum of 1500 down to 800 or less. In our system, the amplifier cards are operated at -4.8 V, resulting in a gain of 1100 and a lower operating temperature for the cards. At this setting, there is a 0.3 mV threshold which produces differential ECL logic pulses of 1.2 V at the end of the 70 meter cable. The cables are Ansley 101-wire flat polyethylene cables with every third wire grounded.

The TDC system, shown schematically in Figure 1, was designed and manufactured at UCLA for this experiment. It digitizes the drift times and encodes the addresses of those wires in the system whose signals arrive during an 80 nsec Level 1 trigger gate. It provides a high-speed path for transfering the wire adresses and drift times to central Randem Access Memory (RAM) on receipt of a Level 2 trigger signal from the experiment. Finally, it makes its own Level 3 trigger decision based on multiplicity logic on the chamber hit data. The Level 3 decision is the computer interrupt.

The TDC cards also have 32 channels so that there is a one-to-one correspondance between TDC and amplifier cards. Up to sixteen TDC cards are mounted in a 19" crate along with their read out module, although a slave crate with up to eight additional modules can also be read out serially by the READOUT module for the larger chamber planes.

The time digitization is accomplished by latching the state of a 4-bit Gray-code counter at the arrival time of a chamber pulse. The Gray-code signals in a given crate are generated by a central clock started by a Level 1 signal from the scintillation hodoscope upstream of the spectrometer. The time bins are 5 nsec wide. Only one "hit" per wire can be registered for each event.

There are 40 READOUT modules, one for each of the wire planes in the system. After an event has been gated into the TDC's, the Level 2 trigger logic either causes the event to be strobed into the MEMORY modules or the entire system is reset. On receiving a good Level 2 ("start readout") signal, the addresses of the wires hit and the digitized times are strobed into the MEMORY modules at the rate of 75 ns/hit with all 40 planes read out in parallel. The total time after a good Level 2 signal to

read out all TDC modules to the MEMORY modules is typically 375 nsec for a 5 track event.

There are 20 MEMORY modules, each of which receives data from a pair of wire planes in the upper and lower spectrometers. Each MEMORY module counts the number of wires hit in each plane of the pair separately as the data is received, and compares the hit counts with upper and lower limits which have been previously down-loaded to the modules from the PDP-11 data aquisition computer. Each module also compares the sum of hits from both pairs to a set of upper and lower limits (each plane in the system has its own set of limits). At the end of the readout process, the results of these comparisons for all MEMORY modules are transferred to a hard-wired processor module called VIRTUS (Very Intelligent Real Time Uvent Selector) which carries out the Level 3 majority logic.

4. SYSTEM PERFORMANCE

Because of the large size of the system (77,366 IC's), there was initial concern that normal failure rates would make smooth, reliable data acquisition difficult. Experience has shown that this is not the case. The hardware in the system works well. Typically, there are 20 channels dead at the amplifier card level. Perhaps once or twice a month, a TDC board (or more likely one of the 41 switching supplies that power them) develops a problem. They are easily replaced by spare modules.

The typical drift velocity of 50 μ/ns implies that the time spread of hits in the chambers should be around 30 nsec. A histogram of raw hits recorded on a typical wire for 1000 events (figure 4) shows that most hits occur within 5 or 6 time bins, as expected. Variations from the nominal 5-nsec time bins have been calibrated with a computer-controlled pulser in order to correct for the effects of imperfections in the Gray-code transmission lines.

The small tail at large times in Figure 4 is due mainly to late arrivals from tracks which pass midway between two neighboring sense wires. The drift time-distance dependence has been studied by using tracks which have zero drift time in an X-plane wire over a large range of incident angles. The calculated traversal point in its neighboring X'-plane is compared with the drift time information from the struck wire in that plane. The results are shown in Figure 5, which is seen to be linear up to about 1.25 mm from the wire. The last .25 mm or so, where the curve levels off, corresponds to the very low field region seen in Figure 2. The observed non-linearity presents no analysis problems - large times correspond to

large distances - but it is necessary that the Level-1 gate be long enough to have full efficiency. Our measured chamber efficiency is typically 99% with the 80 nsec gate.

About 5% of the time, a particle will cause two adjacent wires to fire (i.e. a cluster). Figure 6 is a scatter plot of the times (in units of tdc bins) for the two adjacent wires in two-wire clusters. It can be seen that both hits have times which lie in the tail of figure 4. Most clusters then result when a track passes through the low field region (see fig. 2) near a cell boundary. (Other mechanisms such as δ-ray production or the presence of a nearby track would usually result in a short time for at least one of the wires. This fact is useful since it allows immediate resolution of the left-right ambiguity (discussed below) of any 2-wire cluster. Closer examination of events in Figure 6 in which both recorded times were less than 30 nsec shows that these are mainly due to the presence of a second track.

5. OFFLINE ANALYSIS

The offline pattern recognition program finds tracks using only the wire hit information. The momentum is then determined by fitting to the coordinates determined from the drift-time information. The spatial resolution can be illustrated in the following way. Consider the hits in the X and X' planes for one track crossing a particular chamber. The time information can be used to calculate the distances, d_1 and d_2 respectively, of the track from the hit wires in these planes (see Figure 7). If we assume that the track passes on particular sides of its two wires, d_2 can be predicted using the known slope and the measured distance d_1. Figure 7 also shows a histogram of the difference between the predicted and measured d_2 for all hits in one chamber for the case where the track has been assumed to pass on the right side of both wires. The peak centered at zero comes from those instances where this assumption was correct, while the shoulder at larger values contains all the cases where the assumption was wrong. The width of the peak is $\sqrt{2}$ times the actual resolution which is typically $\sigma = 180\ \mu$. The relative areas of peak and background in Figure 7 depends on the relative offsets of the X and X' planes and on the angular distribution of the tracks used. A direct measurement of the momentum resolution is shown in Figure 8, which is a histogram of the reconstructed antiproton momentum in elastic scattering at 26.7 Gev. This distribution has $\sigma p/p = 5.8\%$.

Finally we comment on the question of left-right ambiguity resolution with our system. The solution of the left-right ambiguity in any given

plane requires that we can predict, using all the available information for a track, where it passed through that plane. The ambiguity will be solved if one and only one of the two possible solutions is consistent with the data from all the other planes.

We solve the ambiguity problem in two steps. First we calculate the track trajectory using only the coordinates of the hit wires. This gives us, to good approximation, the local direction cosines of the track at each chamber pack. The ambiguities are then simultaneously solved for all four planes in a chamber by exploiting the two constraints which relate the four measurements of the track coordinates in the chamber pack. This is done by considering each of the 16 possible solutions. If only one combination satisfies the two constraints, all four ambiguities are solved. If two or more solutions satisfy the constraints, then the ambiguities for one or more planes remain unsolved, depending on the specific combinations.

Using this technique, typically 84% of the cases have at least one X or X' ambiguity solved and about 44% have both solved. Hits for which the ambiguity is not solved are usually those where the drift distance is small ($< 400\mu$), but these cases are unimportant as we already know that the track passed close to the wire. Typically 44% of y-view ambiguities and 56% of u-view ambiguities are solved.

We have attempted to resolve the remaining unsolved ambiguities with a global track fit to the 20 hits in the 5 chamber, using the drift-distance corrected coordinates for those hits whose ambiguities were solved using the method described above. We observed only a small improvement in chamber 2 and no improvement elsewhere. This is because at the chamber level, our track measurements are not highly over-constrained; a different choice of solution results in slightly different track parameters, and not necessarily a different χ^2 for the fit. This illustrates the need for redundant coordinate measurements in a chamber pack if a high efficiency of ambiguity resolution is to be obtained.

The time-distance relationship and the resolution are systematically controlled in the experiment using straight tracks recorded with the ISR operating but with the spectrometer magnet turned off.

6. ACKNOWLEDGEMENTS

We very much appreciate the excellent work at S.T.I.P.E (Saclay) in the design and construction of the chambers. We are grateful to the U.S. National Science Foundation and to the UCLA Physics Department for the support which allowed the development of the chamber electronics. We thank CERN and the ISR Experimental Support Group for their important help in setting up the entire system. P.E.S. thanks Bruce Knapp and Bill Sippach for many invaluable discussions on their experiences with Mini-Drift.

Figure Captions

1. Layout of the R608 spectrometer.

2. The electric field distribution around one anode wire.

3. Block diagram of the chamber TDC and readout system.

4. A histogram of the times recorded in the TDC's of one chamber.

5. The time/distance relationship obtained from fitted tracks.

6. A scatter plot of the times recorded when two neighbouring wires both register hits (for hits used on found tracks).

7. An illustration of the method employed to measure the resolution.

8. Measured momentum distribution of elastic antiprotons at 26 Gev.

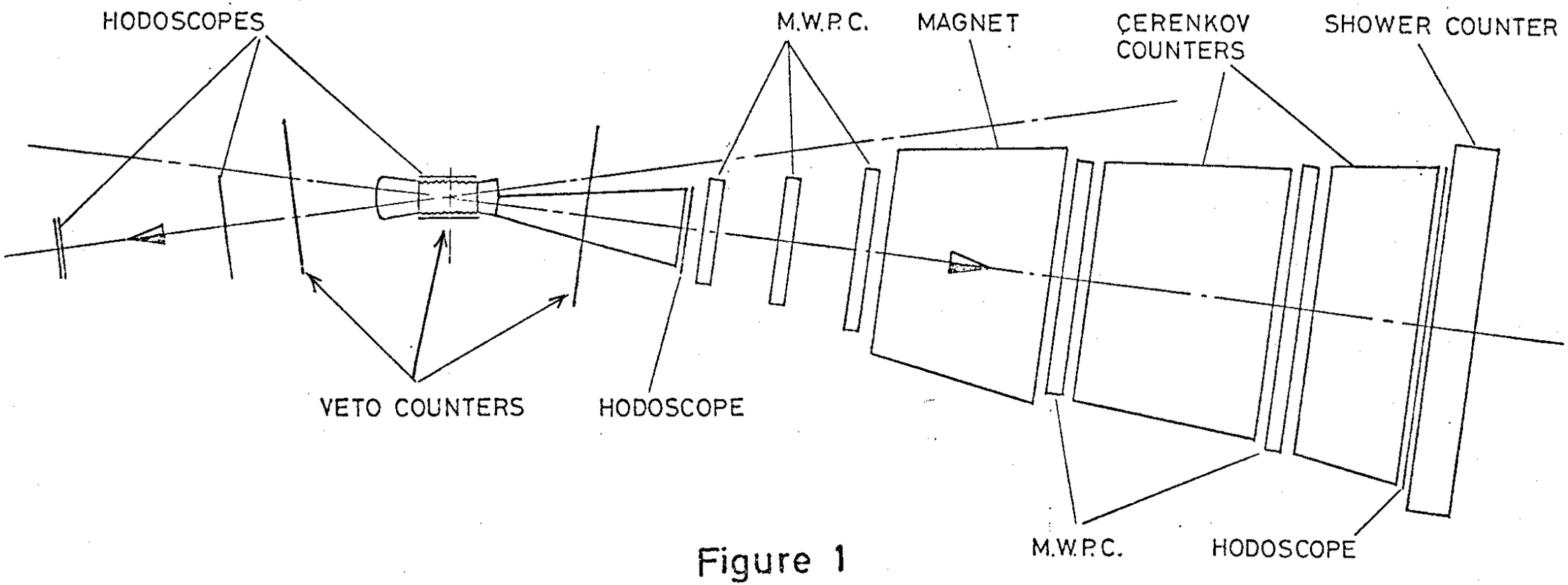
HODOSCOPES
M.W.P.C.
MAGNET
ÇERENKOV COUNTERS
SHOWER COUNTER
VETO COUNTERS
HODOSCOPE
M.W.P.C.
HODOSCOPE

Figure 1

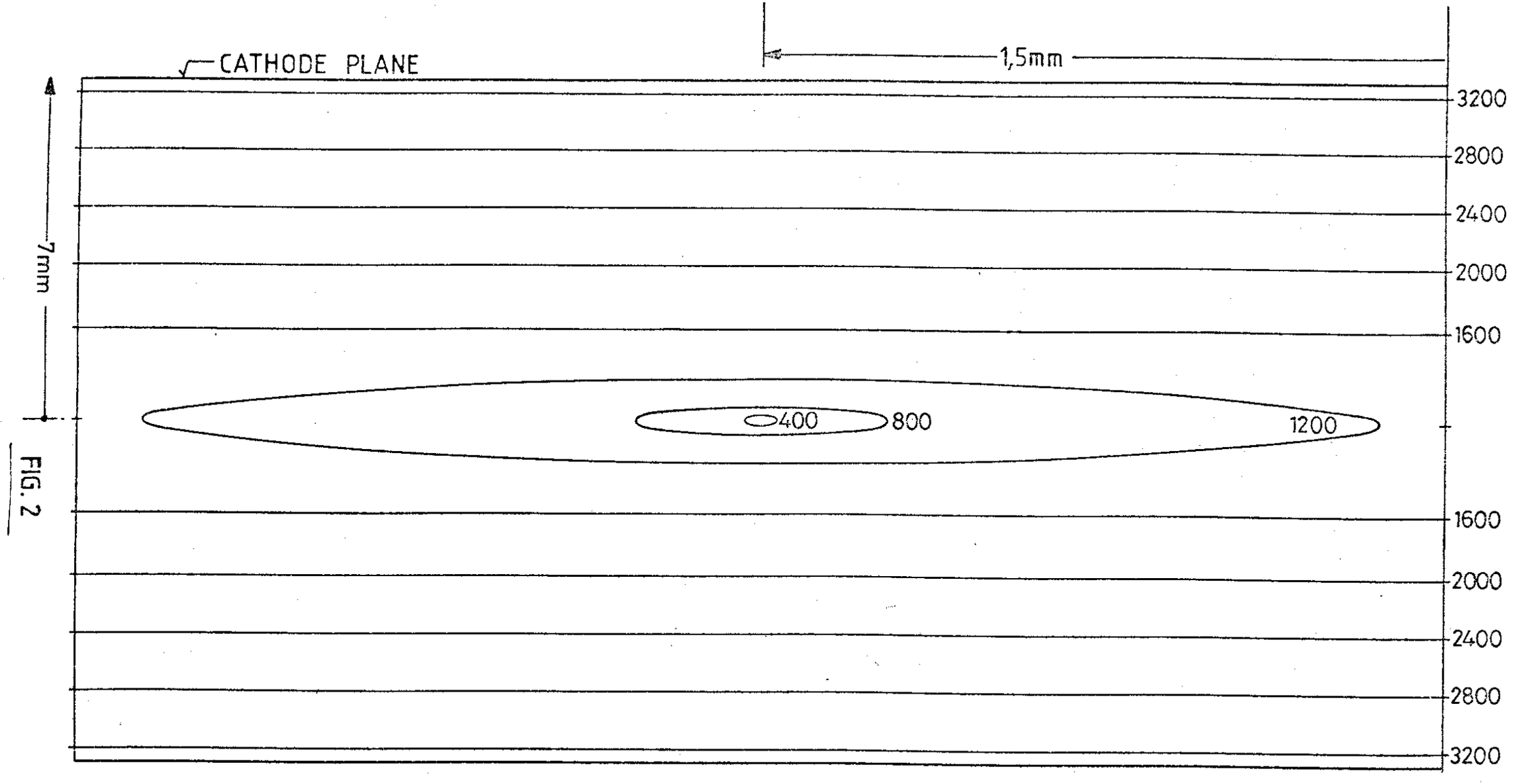

FIG. 2

FIELD DISTRIBUTION
3mm WIRING SPACING

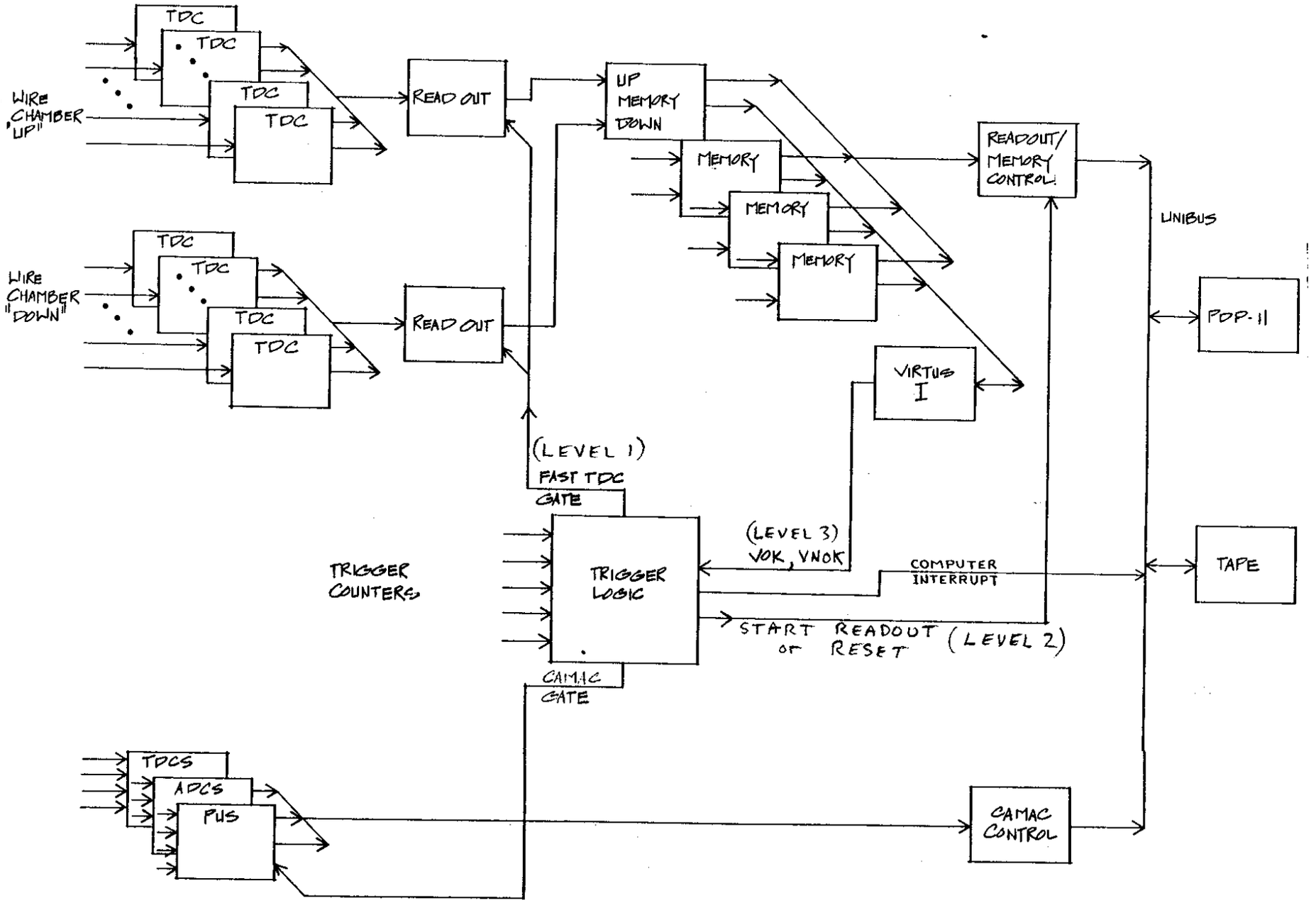
TDC
TDC
TDC
TDC
WIRE CHAMBER "UP"
READ OUT
UP MEMORY DOWN
MEMORY
MEMORY
MEMORY
READOUT/ MEMORY CONTROL
UNIBUS
PDP-11
TDC
TDC
TDC
TDC
WIRE CHAMBER "DOWN"
READ OUT
VIRTUS I
(LEVEL 1)
FAST TDC GATE
TRIGGER COUNTERS
TRIGGER LOGIC
(LEVEL 3) VOK, VNOK
COMPUTER INTERRUPT
TAPE
START READOUT or RESET (LEVEL 2)
CAMAC GATE
TDCS
ADCS
PHS
CAMAC CONTROL

FIG. 3

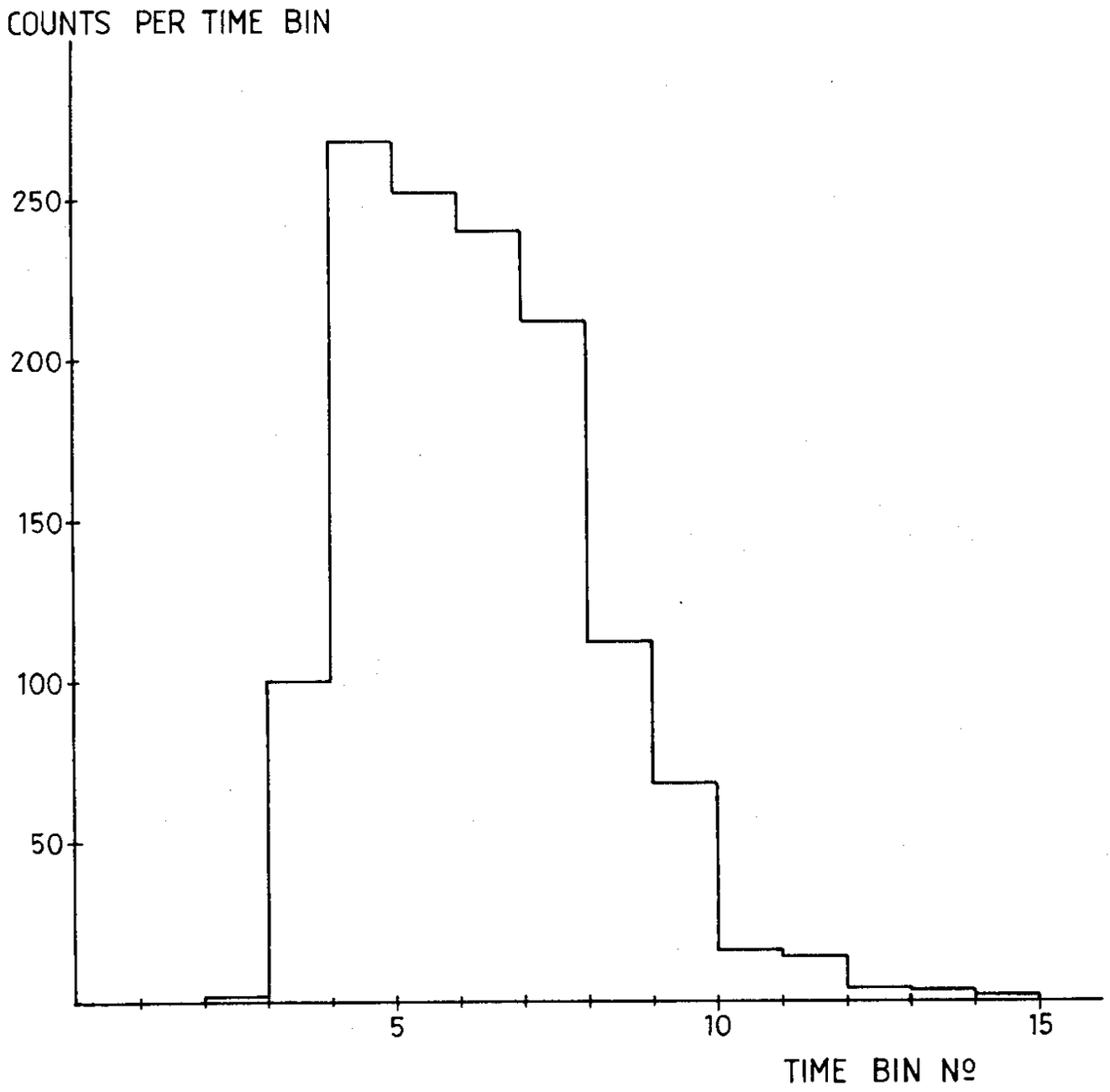

FIG. 4

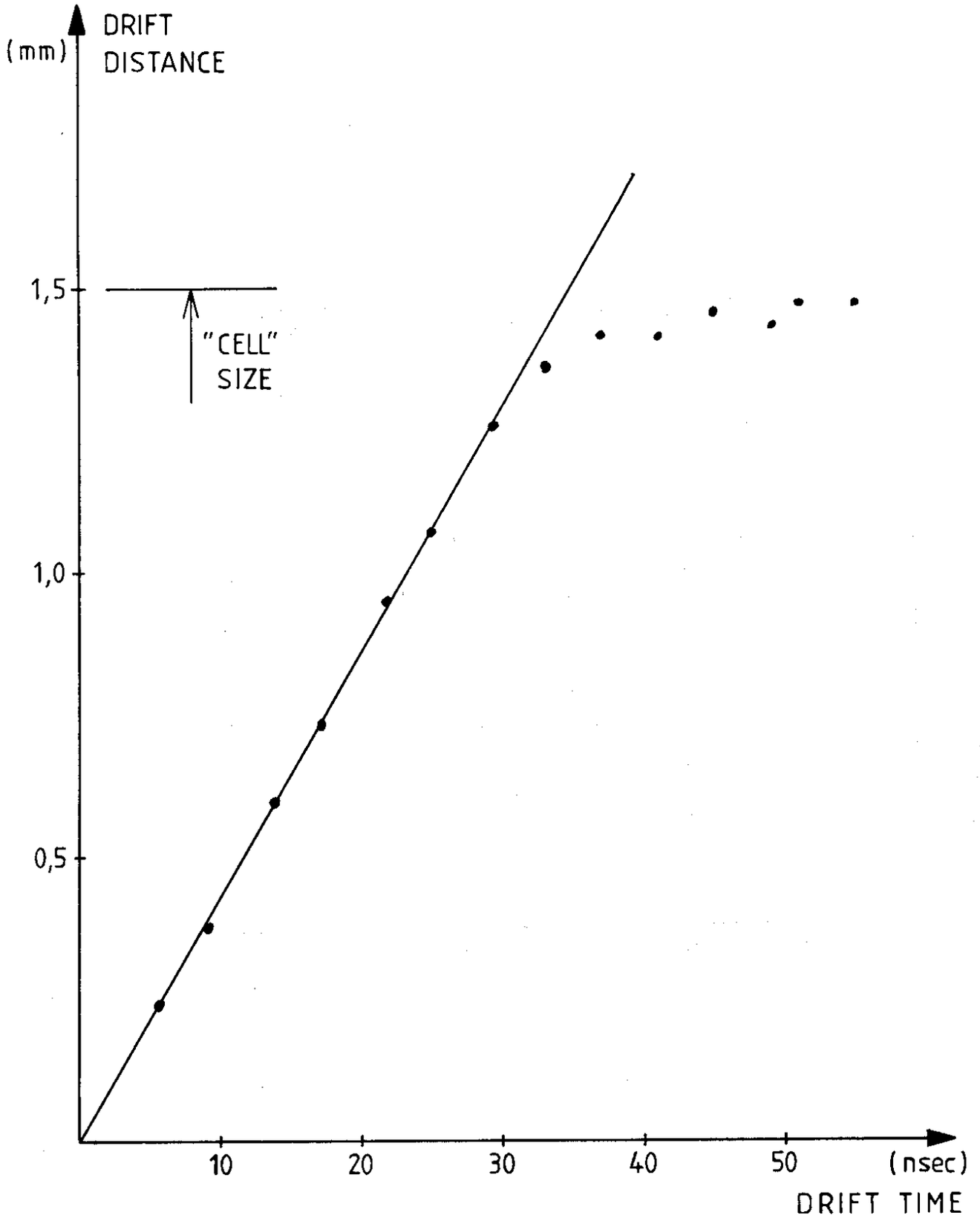
DRIFT
DISTANCE
(mm)
1,5
1,0
0,5
"CELL"
SIZE
10
20
30
40
50
(nsec)
DRIFT TIME

FIG. 5

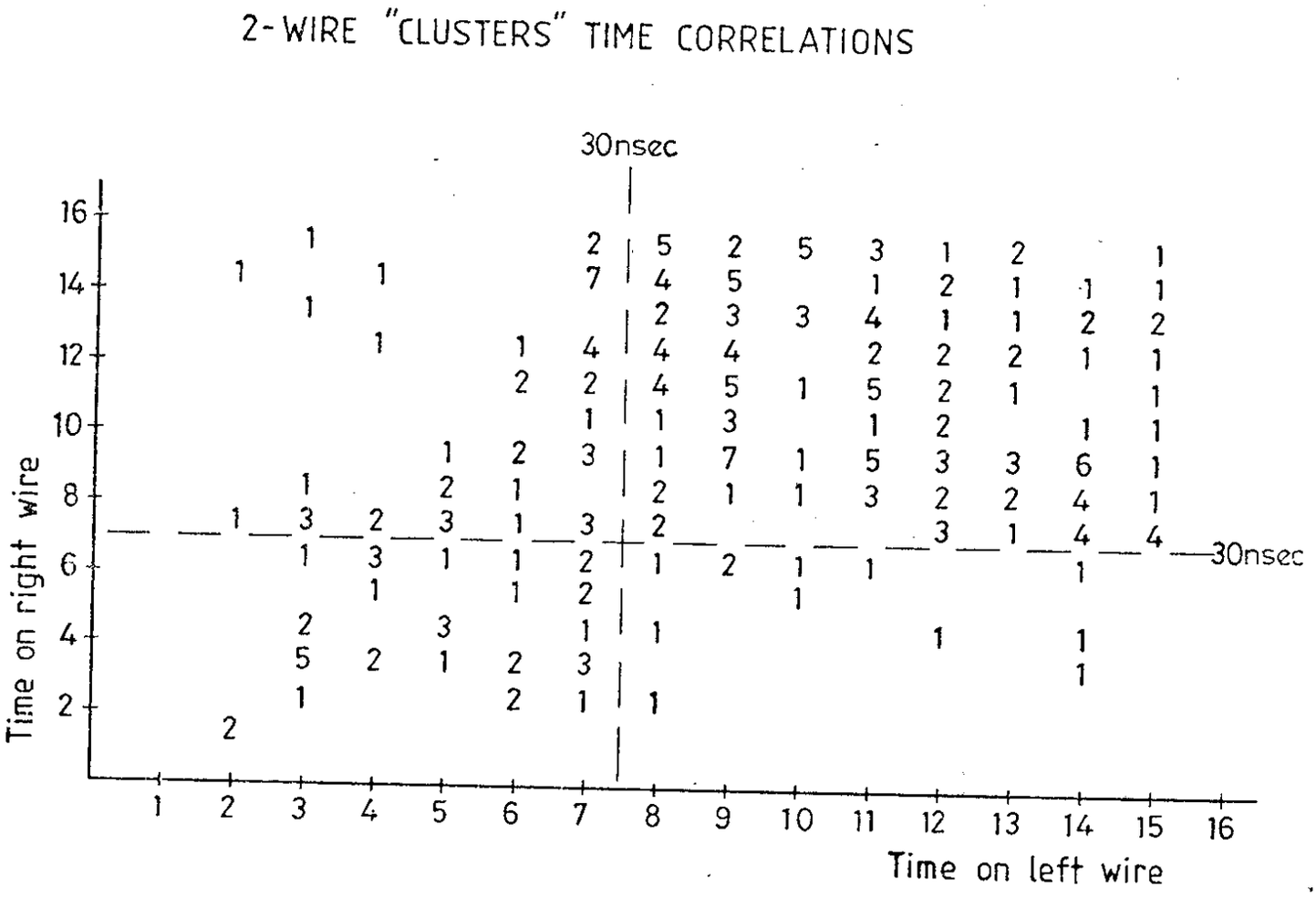
2-WIRE "CLUSTERS" TIME CORRELATIONS
30nsec
Time on right wire
Time on left wire
30nsec
16
14
12
10
8
6
4
2
1
2
3
4
5
6
7
8
9
10
11
12
13
14
15
16

FIG. 6

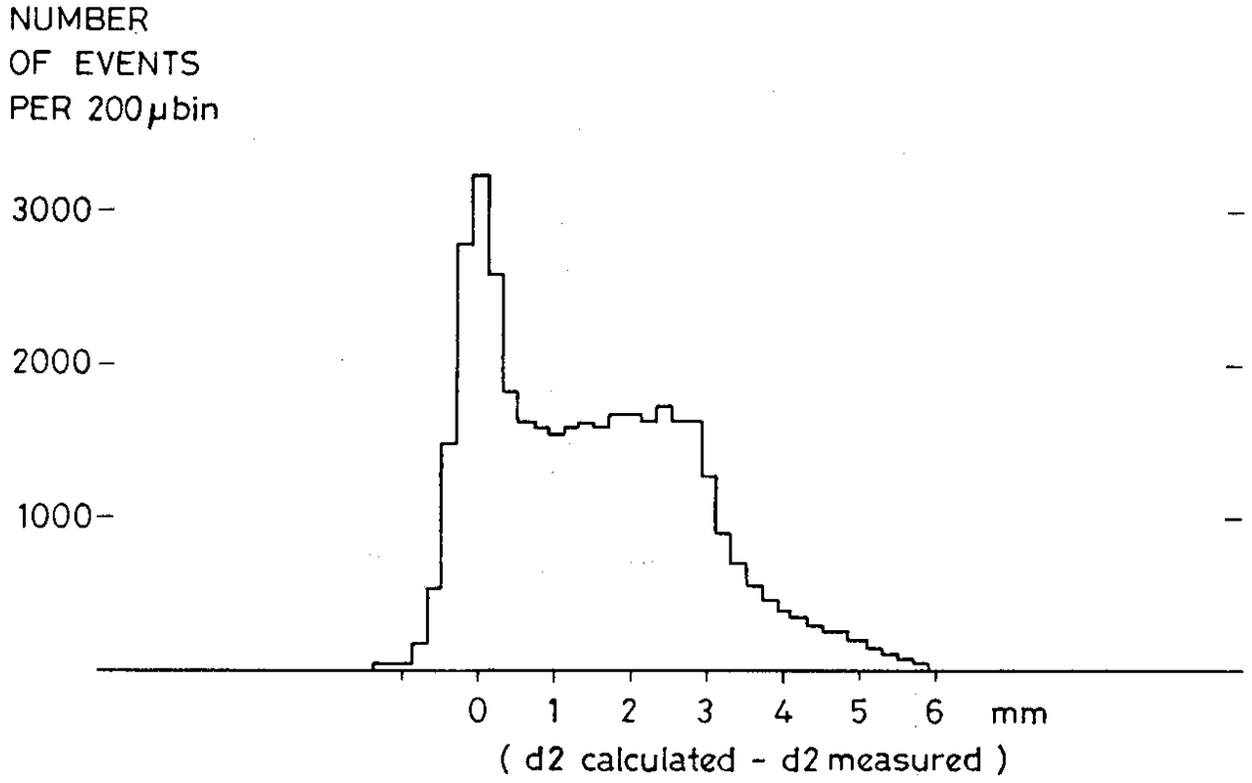
NUMBER
OF EVENTS
PER 200 μ bin
3000
2000
1000
0
1
2
3
4
5
6
mm
(d2 calculated - d2 measured)

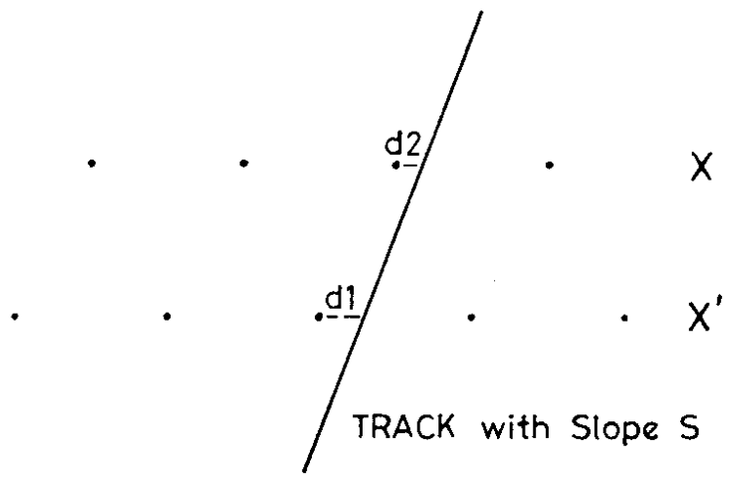
d2
X
d1
X'
TRACK with Slope S

FIG. 7

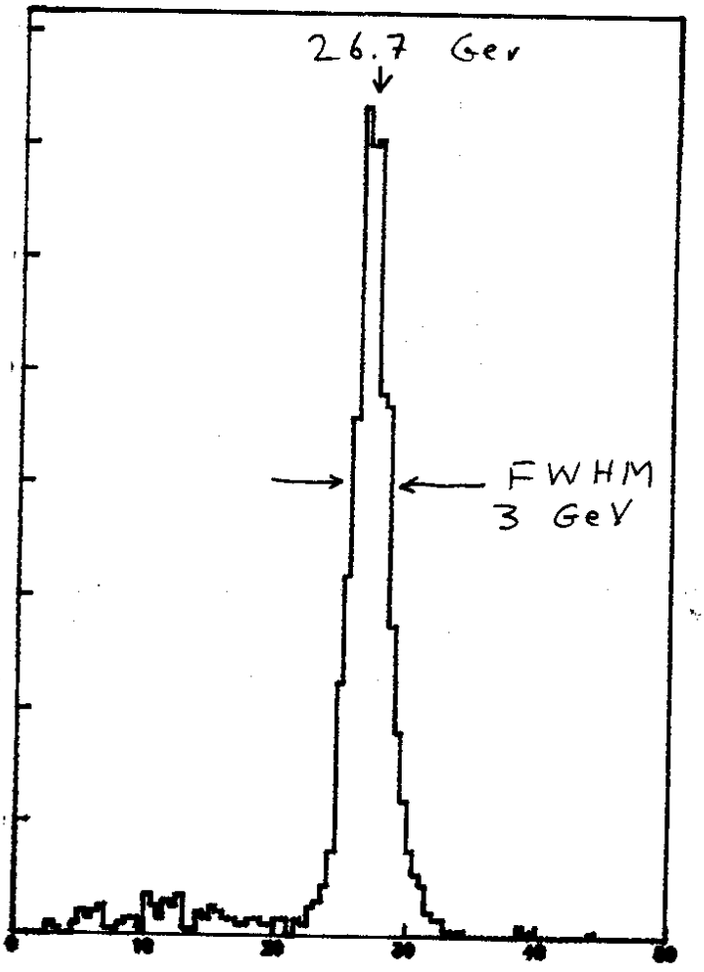

$\bar{p}$ MOMENTUM (GEV/c)

FIG. 8